

Task-Prior Conditional Variational Auto-Encoder for Few-Shot Image Classification

Zaiyun Yang

zy_dimory@stu.xjtu.edu.cn

Abstract. Transductive methods always outperform inductive methods in few-shot image classification scenarios. However, the existing few-shot methods contain a latent condition: the number of samples in each class is the same, which may be unrealistic. To cope with those cases where the query shots of each class are nonuniform (i.e. nonuniform few-shot learning), we propose a Task-Prior Conditional Variational Auto-Encoder model named TP-VAE, conditioned on support shots and constrained by a task-level prior regularization. Our method obtains high performance in the more challenging nonuniform few-shot scenarios. Moreover, our method outperforms the state-of-the-art in a wide range of standard few-shot image classification scenarios. Among them, the accuracy of 1-shot increased by about 3%.

Keywords: Transductive Few-shot Learning; Deep Conditional Variational Auto-encoder; Image Classification

1 Introduction

Deep learning achieves major success in visual classification. Especially the transformer model [6,23] and the paradigm of contrastive learning [3,10] set off a wave in computer vision field. However, these models and paradigms often require large amounts of data, which are unavailable in some image classification scenarios. A human can easily learn a new task rapidly with a handful of examples compared with a machine. To bridge the gap between machine and human, a new paradigm few-shot learning [25,7,37] emerges. In few-shot settings, a model is trained on the base-training set with base classes, and then we generate many few-shot tasks from the testing set with novel classes unseen during training. Each task contains some unlabeled samples (query shots) and one labeled sample (support shot). We evaluate our TP-VAE model performance over the few-shot tasks.

Meta learning based method is a representative paradigm to Few-Shot Learning (FSL) solutions. In the meta learning settings, we view the meta training set as a series of independent tasks, and we use support shots and query shots (from the testing set) to simulate generalization difficulties during test times. Many existing approaches [17,36,48,2] view the meta training (base-training) stage as a feature extraction (embedding) process, which projects the data from the raw data space to the latent feature space. In the feature space, we can easily classify

the query shots. In the stage of meta training, a backbone neural network will be trained as a feature extractor.

Several recent works devote to transductive inference for FSL, e.g., [48, 2, 13, 5, 12, 22], among others. In the transductive settings, the unlabeled query shots participate in training during the meta testing phase instead of only one or a few labeled support shots used like inductive methods.

In the transductive few-shot learning scenarios, query shots supply sufficient information to make the classification results better. However, the existing methods of transductive FSL only consider one situation: the number of query shots for each class is the same, e.g., 15 query shots per class. This setting contains a strong prior condition that the proportion of query shots in each class is the same, but this prior is limited for many situations in the real world. For example, in the field of medical imaging, the number of medical images for each type of disease is different. Through experiments, we discover that some existing methods will suffer performance when the proportion of query shots in each class is different. To cope with this problem, we propose a transductive few-shot method combined with a Task-Prior Conditional Variational Auto-Encoder, named TP-VAE. In our method, the task-level prior provides a regularization, constraining the proportion of query shots in each class. The objective consists of two parts: a standard cross-entropy for the support shots, and a task-prior conditional evidence lower bound (ELBO).

Our contributions are summarized as below:

1. We propose TP-VAE for transductive few-shot learning. Our method optimizes the Task-Prior Conditional ELBO of the query shots and the standard cross-entropy of the support shots. We confirm through ablation experiments that each module in our model contributes to the classification results.
2. We propose a more challenging scenario for few-shot learning (i.e. nonuniform few-shot learning). For fair comparison, we simulate two different nonuniform few-shot scenarios. The experiments show that our method can maintain high performance in this more challenging situation.
3. We conduct extensive experiments in standard few-shot scenario, and the results show that in the standard transductive few-shot scenario, TP-VAE outperforms the state-of-the-art methods in various datasets and networks. To our best of knowledge, the TP-VAE has increased an accuracy of 1-shot by about 3%. Meanwhile, we also obtain a slight improvement in 5-shot scenario.

2 Related Work

2.1 Meta Learning

A large body of previous work addresses the few-shots problem in the meta learning framework, which divides the training process into two part, i.e. meta training and meta testing. We learn the model parameters in the meta training stage and enable the model to quickly generalize to new tasks by sharing

learned knowledge with new tasks. Existing methods of meta learning can be generally divided into three categories. Our method is related to two of them: (1) [8,31,28,49,15] propose a series of optimization-based methods. MAML [8] learns a general initialization model by optimizing the second-order gradient so that when the model faces new tasks, it can converge after a few iterations. [44] explains MAML in the perspective of Bayesian inference. Reptile [26] points out that MAML consumes a lot of resources to calculate the second-order Hessian matrix. They propose a fast algorithm that calculates the first-order Jacobi matrix rather than the Hessian matrix to overcome this difficulty in computational cost. (2) Metric based methods [37,32,35,45,41,12,1] map the raw images into a latent feature space, and classify query shots by measuring the distance from support shots. Matching network [37] learns to map small labeled support shots and an unlabeled query shot to their own labels. Prototypical network [32] maps the sample data in each class into a feature space and extract their "mean" to represent the prototype of each class. [1] proposes an infinite mixture prototype to generalized complex data distributions.

2.2 Transductive Few-Shot Learning

Many previous works [48,2,13,5,12,22,14,27,40,9,42] show that transductive few-shot methods can always outperform inductive few-shot methods due to that transductive methods making full use of the information provided by the query shots. TPN [21] proposes a graphical model, which learns to propagate labels between data instances for unseen classes via episodic meta learning. CSPN [20] analyzes the inner bias between query shot and support set and decreased this bias to improve classification accuracy. LaplacianShot few-shot [48] uses spectral clustering and propose the Laplacian regularization method. TIM [2] maximizes the mutual information between query feature and their predict label, and proposes a very fast optimize method for their TIM named TIM-ADM.

2.3 Deep Conditional Variational AutoEncoder

Variational Auto-Encoder (VAE) [16] is a famous paradigm of deep generative models. On the basis of VAE, many different forms of conditional VAE [33,46,24] are applied to a large number of applications in different tasks such as image generation, text generation, and image classification. [33] conditions on the label message, and [24] conditions on prior clustering preferences with pairwise constrain. Inspired by this, we propose a VAE conditioned on support set in the transductive few-shot scenario. The support set contains the mean message of distribution for each cluster (the centroid of each cluster).

3 Task-Prior Variational Auto-encoder

3.1 Problem Formulation

Following [48,2], we are given a labeled training set, $\mathcal{D}_{\text{base}} = \{x_i, c_i\}_{i=1}^{N_{\text{base}}}$, where x_i denotes raw data and c_i denotes the label of x_i with one-hot encode. This

training set is consistent with meta training set. $\mathcal{C}_{\text{base}}$ is the set of labels for $\mathcal{D}_{\text{base}}$. To generate few-shot tasks, we have another dataset $\mathcal{D}_{\text{test}} = \{x_i, c_i\}_{i=1}^{N_{\text{test}}}$, and $\mathcal{C}_{\text{test}}$ is the set of labels for $\mathcal{D}_{\text{test}}$. It is worth noting that $\mathcal{C}_{\text{test}} \cap \mathcal{C}_{\text{base}} = \emptyset$. For each N-way K-shot task, we construct a labeled support set $\mathcal{S} = \cup_{n=1}^N \{x_i^n, c_i^n\}_{i=1}^k$ and an unlabeled query set $\mathcal{Q} = \cup_{n=1}^N \{x_i^n\}_{i=1}^{N_q}$. Both support set \mathcal{S} and query set \mathcal{Q} are the subset of $\mathcal{D}_{\text{test}}$. The number of query shots for each class will be adjusted according to different tasks, which will be discussed in the experimental part.

In the few-shot scenario, $g_\theta(\cdot)$ is the decoder network, and $f_\phi(\cdot)$ denotes the fixed feature-extractor already trained on $\mathcal{D}_{\text{base}}$ with standard cross-entropy. This training is without any complex meta training or specific sampling schemes. \mathcal{X} denote the random variables associated with the raw image data, and $z_i = f_\phi(x_i) \in \mathbb{R}^d$ denote a continuous latent embedding features. $\mathcal{C} \in \{1, \dots, K\}$ correspond to the real labels of the data, and $\mathcal{Y} \in \{1, \dots, K\}$ correspond to the inference predict labels.

We propose our objective function as follows:

$$\min_{\phi, \psi} \mathcal{L}_{\phi, \psi}^{\text{ce}} + \mathcal{L}_{\phi, \psi}^{\text{tpce}} \quad (1)$$

The first part of Eq.1 is a standard cross-entropy of support features :

$$\mathcal{L}^{\text{ce}} = \frac{1}{L} \sum_{l=1}^L \sum_{s=1}^S \sum_{k=1}^K c_{sk} \log p_\psi(y_s = k | z_s^l) \quad (2)$$

The second part of Eq.1 is a Task-Prior Conditional ELBO:

$$\begin{aligned} \mathcal{L}^{\text{tpce}} = \frac{1}{L} & \left[\underbrace{\sum_{k=1}^K \left[\sum_{i=1}^N p_\psi(y_i = k | z_i^l, S) \right]}_{\mathcal{L}_{\text{tp}}; \text{task-prior KL divergence}} \cdot \log \left(\sum_{i=1}^N \frac{p(y_i)}{p_\psi(y_i = k | z_i^l, S)} \right) \right. \\ & \left. + \sum_{i=1}^N \sum_{k=1}^K p_\psi(y_i = k | z_i^l, S) \log p(z_i^l | y_i = k) + \sum_{l=1}^L \sum_{i=1}^N \log p_\theta(q_i | z_i^l) \right] \quad (3) \end{aligned}$$

In the objective function, z_i^l are the embedding features samples.

The distribution of each random variable can be summarized as follows:

$$p_\theta(q_i | z_i) \sim \mathcal{N}(\mu_{q_i}, \sigma_{q_i} \mathbb{I}) \quad (4)$$

$$p(z_i | y_i = k) \sim \mathcal{N}(\mu_{y_i=k}, \sigma_{y_i=k}^2 \mathbb{I}) \quad (5)$$

$$p_\psi(y_i = k | z_i) \sim \text{Cat}(k) \quad (6)$$

Where $[\mu_{q_i}, \sigma_{q_i}^2 \mathbb{I}]$ is obtained by decoder $g_\theta(\cdot)$, and $[\mu_{y_i=k}, \sigma_{y_i=k}^2 \mathbb{I}]$ represents the mean and variance of the Gaussian distribution corresponding to k th cluster in feature space when $y_i = k$. ψ represent a classifier initialed by support embedding features z_s . We do inference about the posterior distribution $p_\psi(y_i | z_i)$

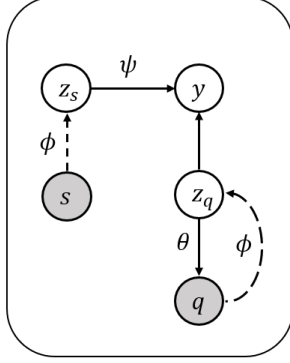


Fig. 1. Graphical model for TP-VAE. The dashed line denotes the variational approximation process. The solid lines denote generate process and prototype nearest-neighbor inference process

by prototype nearest-neighbor classification [39]. The specific inference process is as follows:

Initialize the classifier:

$$\psi_k^{(0)} = \frac{\sum_{i \in s} c_{ik} z_i}{\sum_{i \in s} c_{ik}} \quad (7)$$

Then the mean of k th Gaussian distribution equals ψ_k , i.e. $\psi_k = \mu_{y_i=k}$.

After prototype nearest-neighbor classification [39], we can obtain the following relation:

$$p(z_i | y_i = k) \propto \exp\left(\frac{-(z_i - \psi_k)^2}{\sigma^2}\right) \quad (8)$$

$$p_\psi(y_i = k | z_i) \propto \frac{\exp\left(\frac{-(z_i - \psi_k)^2}{\sigma^2}\right)}{\sum_{j=1}^k \exp\left(\frac{-(z_i - \psi_j)^2}{\sigma^2}\right)} \quad (9)$$

About the prior $p(y_i)$, We take the result of the first classification result by untrained classifier ψ_k (support feature) as our prior:

$$p(y_i) = p_\psi^{(1)}(y_i = k | z_i) \quad (10)$$

The graphical illustration of TP-VAE is depicted in Fig. 1, and we detail algorithm of TP-VAE in Algorithm 1.

Algorithm 1: Proposed Algorithm for TP-VAE

Data: \mathcal{S}, \mathcal{Q}

Output: posterior distribution $p_\psi(y_i = k|z_i)$

- 1 initialize θ randomly;
 - 2 initialize ψ using (7);
 - 3 computer ϕ at the stage of base-training;
 - 4 compute $p(y_i)$ using (10);
 - 5 **while** *not done* **do**
 - 6 sampling z_i^l from $q_\phi(z)$;
 - 7 compute $p_\psi(y_i = k|z_i)$ using (9);
 - 8 compute \mathcal{L}_{tpe} using (3);
 - 9 optimize \mathcal{L}_{tpe} using SGD;
 - 10 **end**
-

3.2 Task-Prior Conditional ELBO

The log-likelihood of the query data can be written as follows:

$$\log p(\mathcal{Q}|\mathcal{S}) = \log \frac{p(\mathcal{Q}, Z, Y|\mathcal{S})}{p(Z, Y|\mathcal{Q}, \mathcal{S})} \quad (11)$$

$$= \mathbb{E}_{q_{\phi, \psi}(Z, Y|\mathcal{Q}, \mathcal{S})} \log \frac{p(\mathcal{Q}, Z, Y|\mathcal{S})}{p(Z, Y|\mathcal{Q}, \mathcal{S})} \quad (12)$$

$$= \mathbb{E}_{q_{\phi, \psi}(Z, Y|\mathcal{Q}, \mathcal{S})} \log \frac{p(\mathcal{Q}, Z, Y|\mathcal{S})}{q_{\phi, \psi}(Z, Y|\mathcal{Q}, \mathcal{S})} \quad (13)$$

$$+ \mathbb{E}_{q_{\phi, \psi}(Z, Y|\mathcal{Q}, \mathcal{S})} \log \frac{q_{\phi, \psi}(Z, Y|\mathcal{Q}, \mathcal{S})}{p(Z, Y|\mathcal{Q}, \mathcal{S})}$$

Where $Z = \{z_i\}_{i=1}^N$ are the latent embedding features associated with the query shots. $Y = \{y_i\}_{i=1}^N \in \{1, 2, \dots, k\}$ are the latent predict label. The first term of Eq.13 is a conditional ELBO of the marginal likelihood. The second term is a KL divergence. When $q_{\phi, \psi}(Z, Y|\mathcal{Q}, \mathcal{S}) = p(Z, Y|\mathcal{Q}, \mathcal{S})$, the ELBO equals the marginal likelihood.

The conditional ELBO can be written as follows:

$$\mathcal{L}^{cpe} = \mathbb{E}_{q_{\phi, \psi}(Z, Y|\mathcal{Q}, \mathcal{S})} \log \frac{p(\mathcal{Q}, Z, Y|\mathcal{S})}{q_{\phi, \psi}(Z, Y|\mathcal{Q}, \mathcal{S})} \quad (14)$$

$$= \mathbb{E}_{q_{\phi, \psi}(Z, Y|\mathcal{Q}, \mathcal{S})} \log p_\theta(\mathcal{Q}|Z) + \mathbb{E}_{q_{\phi, \psi}(Z, Y|\mathcal{Q}, \mathcal{S})} \log \frac{p(Z, Y|\mathcal{S})}{q_{\phi, \psi}(Z, Y|\mathcal{Q}, \mathcal{S})} \quad (15)$$

$$= \mathbb{E}_{q_\phi(Z|\mathcal{Q})} \log p_\theta(\mathcal{Q}|Z) + \mathbb{E}_{q_\phi(Z|\mathcal{Q})} p_\psi(Y|Z, \mathcal{S}) \log p(Z|Y) \quad (16)$$

$$+ \mathbb{E}_{q_\phi(Z|\mathcal{Q})} p_\psi(Y|Z, \mathcal{S}) \log \frac{p(Y)}{p_\psi(Y|Z, \mathcal{S})} - \mathbb{E}_{q_\phi(Z|\mathcal{Q})} \log q_\phi(Z|\mathcal{Q})$$

When $q_\phi(Z|\mathcal{Q})$ is Gaussian, the last part of Eq.16 can be factorized as follows:

$$\mathbb{E}_{q_\phi(Z|\mathcal{Q})} \log q_\phi(Z|\mathcal{Q}) = -\frac{D}{2} \log(2\pi) - \frac{1}{2} \sum_{d=1}^D (1 + \log \sigma_d^2) \quad (17)$$

Where d represents the dimension of the Gaussian distribution. When we set σ_j^2 to a constant, Eq.17 becomes a constant. Then we remove it from the objective function.

Given $q_\phi(Z|\mathcal{Q})p_\psi(Y|Z, \mathcal{S}) = \prod_{i=1}^N q_\phi(z_i|q_i)p_\psi(y_i|z_i, s_i)$, we use the Monte Carlo sampling method to sample z_i from $q_\phi(z_i|q_i)$, \mathcal{L}^{cpe} can be factorized as follows:

$$\begin{aligned} \mathcal{L}^{cpe} = & \frac{1}{L} \sum_{l=1}^L \left[\sum_{i=1}^N \log p_\theta(q_i|z_i^l) + \sum_{i=1}^N \sum_{k=1}^K p_\psi(y_i = k|z_i^l, S) \log p(z_i^l|y_i = k) \right. \\ & \left. + \sum_{i=1}^N \sum_{k=1}^K p_\psi(y_i = k|z_i^l, S) \log \frac{p(y_i)}{p_\psi(y_i = k|z_i^l, S)} \right] \end{aligned} \quad (18)$$

The third part of the Eq.18 is a KL divergence between the posterior distribution $p_\psi(y_i|z_i)$ and prior $p(y_i)$. As mentioned above, we calculate prior from Eq.10. However, if we just optimize the KL divergence at the sample level (every query shot is regularized by the prior), the classification result will stay in the first classification result and can't converge to a better result. For our model converge to a better results, we use the Jensen inequality to lighten the constraint of the sample level KL divergence. Then we obtain a task level KL divergence: proportion of query shots in each class are regularized by the prior (e.g., if the category of cats in the first classification accounts for 30% of the total categories, We should regularize the proportion of cat category to 30% in the prior). Then we can obtain the Task-Prior Conditional ELBO as follows:

$$\begin{aligned} \mathcal{L}^{cpe} \geq & \frac{1}{L} \left[\sum_{l=1}^L \sum_{i=1}^N \log p_\theta(q_i|z_i^l) + \sum_{i=1}^N \sum_{k=1}^K p_\psi(y_i = k|z_i^l, S) \log p(z_i^l|y_i = k) \right. \\ & \left. + \sum_{k=1}^K \left[\sum_{i=1}^N p_\psi(y_i = k|z_i^l, S) \right] \cdot \log \left(\sum_{i=1}^N \frac{p(y_i)}{p_\psi(y_i = k|z_i^l, S)} \right) \right] = \mathcal{L}^{\text{tpce}} \end{aligned} \quad (19)$$

4 Experiments

This section provides our experiment setup details for the few-shots image classification. We report the average of accuracies evaluated over 1000 episodes in all our experiments.

4.1 Datasets

We use three standard benchmarks for few-shot image classification: *mini-ImageNet* [37], *tiered-ImageNet* [30], and *cub-200-2011* [38].

Mini-ImageNet has 60000 color images with 100 classes. Following previous work [29,39], we divide the dataset into 64 bases, 16 validations and 20 test classes.

Tiered-ImageNet has large data with 608 classes. Following [30], we divide the dataset into 351 bases, 97 validations and 160 test classes.

CUB-200-2011 is a fine-grained dataset. We follow [4] splitting the dataset into 100 bases, 50 validations and 50 test classes for the experiments.

4.2 Hyper-Parameters

We keep the hyper-parameter fixed across all the models and datasets to make our experiments easier to implement. The label-smoothing parameter is set to 0.1 during the meta training stage. When we implement our TP-VAE, the learning rate of the SGD optimizer is set to 1×10^{-1} with momentum 0. The number of samples l is set to 1. Inverse of variance always be seen as a temperature parameter τ in many contrastive learning and few-shot learning scenarios [2,39,18]. We choose appropriate temperature parameters in the ablation experiments.

4.3 Base-Training Procedure

We evaluate TP-VAE on two different backbone networks models as the feature extractor f_ϕ : ResNet-18 [11] is the most common neural networks used in deep learning, which has 8 basic residual blocks. WRN-28 [47] has more convolutional layers and feature planes, which often achieve better results than ResNet-18 as a feature extractor. As for the decoder neural network g_θ , we use a simple Conv-4 network [37].

For a fair comparison with previous works, our feature extractor is trained following LaplacianShot and TIM [48,2]. We train the feature extractor using the standard cross-entropy with label smoothing. It is worth mentioning that the base training stage doesn't involve any other complex meta learning or episodic-training strategy. We use the SGD optimizer to train the feature extractor with an early stopping strategy, and we set 256 batch sizes for ResNet-18 and 128 batch sizes for WRN-28. About data augment, we use random cropping, color jitter and random horizontal flipping like [48,2].

4.4 TP-VAE Implement

We implement our TP-VAE as described in Algorithm 1. We record the training process of TP-VAE on three benchmark datasets with ResNet-18. The results are recorded in Fig. 2. It can be observed that our method can achieve high performance at 200 episodes and converge within 1000 episodes on all datasets.

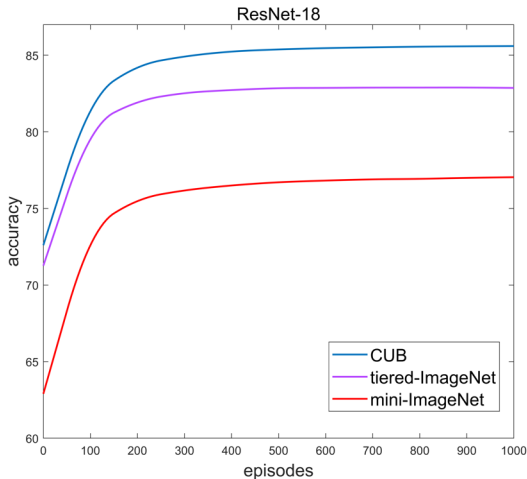


Fig. 2. The accuracy improvement trend during the training process

4.5 Comparison Results with the State-of-The-Art Methods

We evaluate our TP-VAE in the standard 5-way 1-shot and 5-way 5-shot scenarios with *15 query shot for each class* (total 75 query shots) on the Mini-ImageNet, tired-ImageNet, and CUB-2011. The results are reported in Table 1 and Table 2. TP-VAE can achieve the state-of-the-art performances by a large margin, with different network models and datasets. For instance, compared with LaplacianShot and TIM, TP-VAE outperforms 5% and 3% respectively in 1-shot scenario. To illustrate our model can be widely applied to few-shot learning, not just limited to the 5-way scenario, we also do experiments on more challenging 10-way and 20-way scenarios. The results are reported in Table 3. Our method also achieves the state-of-the-art in this more challenging scenario.

4.6 TP-VAE for Nonuniform Few-shot Image Classification

In order to simulate the situation that the number of samples of different categories in the real world is not uniform, we simulate two different situations:

1. The proportion of query shots in each class is slightly different (we set the number of query shots to [20, 20, 10, 10, 15]).
2. The number of query shots in one class is extremely small ([19, 19, 18, 18, 1]).

We compare our method with TIM [2] and LaplacianShot [48] on *mini-ImageNet*, *tiered-ImageNet*, and CUB-200-2011 with ResNet-18. The main results are shown in Table 4 and Table 5. In these two simulation scenarios, the performance of TIM is greatly affected, which indicates that TIM method potentially exploits the strong uniform prior condition. In comparison, our method can maintain high performance in all scenarios. Specifically, compared with TIM and

Table 1. Comparison to the state-of-the-art methods on *mini-ImageNet* and *tiered-Imagenet*. The best performances are shown in **bold**, and ”-” signifies the result is unavailable

Method	Transductive	Backbone	<i>mini-ImageNet</i>		<i>tiered-ImageNet</i>	
			1-shot	5-shot	1-shot	5-shot
MAML [8]	✗	ResNet-18	49.6	65.7	-	-
MatchNet [37]	✗	ResNet-18	52.9	68.9	-	-
ProtoNet [32]	✗	ResNet-18	54.2	73.4	-	-
TPN [21]	✓	ResNet-12	59.5	75.7	-	-
TEAM [27]	✓	ResNet-18	60.1	75.9	-	-
MTL [34]	✓	ResNet-12	61.2	75.5	-	-
Neg-cosine [19]	✗	ResNet-18	62.3	80.9	-	-
MetaOpt [17]	✗	ResNet-12	62.6	78.6	66.0	81.6
SimpleShot [39]	✗	ResNet-18	62.9	80.0	68.9	84.6
Distill [36]	✗	ResNet-12	64.8	82.1	71.5	86.0
CAN+T [12]	✓	ResNet-12	67.2	80.6	73.2	84.9
LaplacianShot [48]	✓	ResNet-18	72.1	82.3	79.0	86.4
TIM[2]	✓	ResNet-18	73.9	85.0	79.9	88.5
TP-VAE (ours)	✓	ResNet-18	76.9	85.2	82.9	89.1
LEO [31]	✗	WRN28-10	61.8	77.6	66.3	81.4
AWGIM [9]	✓	WRN28-10	63.1	78.4	67.7	82.8
SimpleShot [39]	✗	WRN28-10	63.5	80.3	69.8	85.3
MatchNet [37]	✗	WRN28-10	64.0	76.3	-	-
FEAT [43]	✗	WRN28-10	65.1	81.1	70.4	84.4
Ent-min [5]	✓	WRN28-10	65.7	78.4	73.3	85.5
SIB [13]	✓	WRN28-10	70.0	79.2	-	-
LaplacianShot [48]	✓	WRN28-10	74.9	84.1	80.2	87.6
TIM[2]	✓	WRN28-10	77.8	87.4	82.1	89.8
TP-VAE (ours)	✓	WRN28-10	79.8	87.2	84.3	90.2

LaplacianShot fairly, TP-VAE brings about 5% improvement in the nonuniform 1-shot scenario and about 4% improvement in the nonuniform 5-shot scenario.

4.7 Ablation Study

Effects of the task-prior regularization: Our objective function consists of two parts: \mathcal{L}^{ce} and $\mathcal{L}^{\text{tpce}}$. To evaluate the effects of the task-prior regularization, we divide $\mathcal{L}^{\text{tpce}}$ into two parts, the task-prior KL divergence is recorded as \mathcal{L}^{tp} , and the remainder is denoted as \mathcal{L}^{re} . The result reported in Table 6. All the components of our objective function contribute to the final result: the cross-

Table 2. Comparison to the state-of-the-art methods on CUB. The best performances are shown in **bold**, and ”-” signifies the result is unavailable

Method	Transductive	Backbone	CUB-200-2011	
			1-shot	5-shot
MAML [8]	✗	ResNet-18	68.4	83.5
MatchNet [37]	✗	ResNet-18	73.5	84.5
ProtoNet[32]	✗	ResNet-18	73.0	86.6
TPN [21]	✓	ResNet-12	-	-
TEAM [27]	✓	ResNet-18	-	-
MTL [34]	✓	ResNet-12	-	-
Neg-cosine [19]	✗	ResNet-18	72.7	89.4
MetaOpt [17]	✗	ResNet-12	-	-
SimpleShot [39]	✗	ResNet-18	68.9	84.0
Distill [36]	✗	ResNet-12	-	-
CAN+T [12]	✓	ResNet-12	-	-
LaplacianShot [48]	✓	ResNet-18	81.0	88.7
TIM[2]	✓	ResNet-18	82.2	90.8
TP-VAE (ours)	✓	ResNet-18	85.6	91.0

Table 3. Test results for 10-way and 20-way scenarios on *mini*-ImageNet with ResNet-18

Method	10way		20way	
	1-shot	5-shot	1-shot	5-shot
MatchNet[37]	-	52.3	-	36.8
Baseline[4]	-	55.0	-	42.0
ProtoNet[32]	-	59.2	-	45
SimpleShot[39]	45.1	68.1	32.4	55.4
TIM[2]	56.1	72.8	39.3	59.5
TP-VAE (ours)	57.7	73.2	39.5	59.4

Table 4. Test results for extremely non-uniformed few-shot scenario with ResNet-18

Method	<i>mini</i> -ImageNet		<i>tiered</i> -ImageNet		CUB-200-2011	
	1-shot	5-shot	1-shot	5-shot	1-shot	5-shot
LaplacianShot	69.3	80.2	76.1	84.7	78.0	87.0
TIM	64.0	72.6	68.6	75.2	70.5	77.2
TP-VAE	74.1	85.5	81.7	88.9	84.5	91.0

Table 5. Test results for slightly non-uniformed few-shot scenario with ResNet-18

	<i>mini-ImageNet</i>		<i>tiered-ImageNet</i>		CUB-200-2011	
Method	1-shot	5-shot	1-shot	5-shot	1-shot	5-shot
LaplacianShot	69.3	81.4	76.6	85.8	79.0	87.9
TIM	62.7	71.2	67.0	73.6	68.7	75.6
TP-VAE	75.1	85.2	81.6	88.9	84.5	91.0

entropy of the support shot allows us make full use of the information contained in support shots and its labels. The remainder part \mathcal{L}^{re} makes the query shots into a class more confident. The task-prior KL divergence regular constraints the objective function so that the final result is not all query shots are classified into one class.

Choosing the Value of τ : The value of τ denotes the concentration level of the distribution around a centroid. We choose the value of τ in [5, 10, 25, 35, 50, 75, 100] by ablation study with ResNet-18. The results are reported in Fig. 3. The trends of the results are consistent in both 1-shot and 5-shot scenarios. In most cases, $\tau=25$ provides the best results in both 1-shot and 5-shot scenarios. So, we set the value of τ to 25 in all our experiments.

Table 6. Ablation study on the effect of each component in our objective function with ResNet-18

	<i>mini-ImageNet</i>		<i>tiered-ImageNet</i>		CUB-200-2011	
Loss	1-shot	5-shot	1-shot	5-shot	1-shot	5-shot
\mathcal{L}^{ce}	60.2	79.2	68.0	84.7	68.7	86.0
$\mathcal{L}^{\text{ce}}+\mathcal{L}^{\text{re}}$	48.5	73.2	56.6	82.2	57.1	83.9
$\mathcal{L}^{\text{ce}}+\mathcal{L}^{\text{tp}}$	68.0	81.9	75.4	87.2	75.8	88.2
$\mathcal{L}^{\text{ce}}+\mathcal{L}^{\text{tp}}+\mathcal{L}^{\text{re}}$	76.9	85.2	82.9	89.1	85.6	91.0

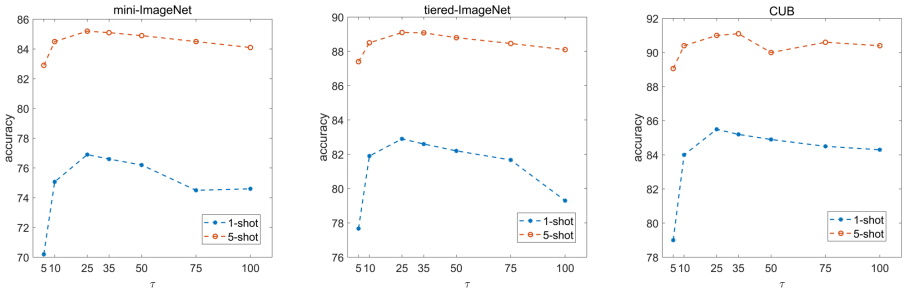


Fig. 3. The results for the ablation study of choosing τ on *mini-ImageNet*, *tiered-ImageNet*, and CUB-200-2011 with ResNet-18

5 Conclusions

We proposed a VAE model conditioned on support shots and relaxed a sample level KL regularization constrain to a task level. Our method obtains the state-of-the-art on a wide range of standard few-shot benchmarks. Especially in the one-shot scenario, our method achieves about 3% improvement compared with previous methods. Besides, we proposed a more challenging scenario for transductive few-shot learning: the query shots of each class are nonuniform. We simulated two nonuniform few-shot scenarios and found that some previous methods suffered performance in this more challenging situation. In comparison, our TP-VAE maintained high performance. Our method has another advantage: TP-VAE is a meta testing module that can connect any base-training module and is a template for researchers to use. In future work, we aim to combine the contrastive learning paradigm, Variational Auto-Encoder paradigm, and few-shot learning paradigm to find a stronger feature extractor and obtain better results.

References

1. Allen, K., Shelhamer, E., Shin, H., Tenenbaum, J.: Infinite mixture prototypes for few-shot learning. In: International Conference on Machine Learning. pp. 232–241. PMLR (2019)
2. Boudiaf, M., Masud, Z.I., Rony, J., Dolz, J., Piantanida, P., Ayed, I.B.: Transductive information maximization for few-shot learning. arXiv preprint arXiv:2008.11297 (2020)
3. Chen, T., Kornblith, S., Norouzi, M., Hinton, G.: A simple framework for contrastive learning of visual representations. In: International conference on machine learning. pp. 1597–1607. PMLR (2020)
4. Chen, W.Y., Liu, Y.C., Kira, Z., Wang, Y.C.F., Huang, J.B.: A closer look at few-shot classification. arXiv preprint arXiv:1904.04232 (2019)
5. Dhillon, G.S., Chaudhari, P., Ravichandran, A., Soatto, S.: A baseline for few-shot image classification. In: International Conference on Learning Representations (ICLR) (2020)
6. Dosovitskiy, A., Beyer, L., Kolesnikov, A., Weissenborn, D., Zhai, X., Unterthiner, T., Dehghani, M., Minderer, M., Heigold, G., Gelly, S., et al.: An image is worth 16x16 words: Transformers for image recognition at scale. arXiv preprint arXiv:2010.11929 (2020)
7. Fei-Fei, L., Fergus, R., Perona, P.: One-shot learning of object categories. *IEEE transactions on pattern analysis and machine intelligence* **28**(4), 594–611 (2006)
8. Finn, C., Abbeel, P., Levine, S.: Model-agnostic meta-learning for fast adaptation of deep networks. In: International conference on machine learning. pp. 1126–1135. PMLR (2017)
9. Guo, Y., Cheung, N.M.: Attentive weights generation for few shot learning via information maximization. In: Proceedings of the IEEE/CVF Conference on Computer Vision and Pattern Recognition. pp. 13499–13508 (2020)
10. He, K., Fan, H., Wu, Y., Xie, S., Girshick, R.: Momentum contrast for unsupervised visual representation learning. In: Proceedings of the IEEE/CVF Conference on Computer Vision and Pattern Recognition. pp. 9729–9738 (2020)
11. He, K., Zhang, X., Ren, S., Sun, J.: Deep residual learning for image recognition. In: Proceedings of the IEEE conference on computer vision and pattern recognition. pp. 770–778 (2016)
12. Hou, R., Chang, H., Ma, B., Shan, S., Chen, X.: Cross attention network for few-shot classification. In: NeurIPS (2019)
13. Hu, S.X., Moreno, P.G., Xiao, Y., Shen, X., Obozinski, G., Lawrence, N.D., Damiou, A.: Empirical bayes transductive meta-learning with synthetic gradients. In: International Conference on Learning Representations (ICLR) (2020)
14. Hu, Y., Gripon, V., Pateux, S.: Leveraging the feature distribution in transfer-based few-shot learning. In: International Conference on Artificial Neural Networks. pp. 487–499. Springer (2021)
15. Jamal, M.A., Qi, G.J.: Task agnostic meta-learning for few-shot learning. In: Proceedings of the IEEE/CVF Conference on Computer Vision and Pattern Recognition. pp. 11719–11727 (2019)
16. Kingma, D.P., Welling, M.: Auto-encoding variational bayes. arXiv preprint arXiv:1312.6114 (2013)
17. Lee, K., Maji, S., Ravichandran, A., Soatto, S.: Meta-learning with differentiable convex optimization. In: Proceedings of the IEEE/CVF Conference on Computer Vision and Pattern Recognition. pp. 10657–10665 (2019)

18. Li, J., Zhou, P., Xiong, C., Hoi, S.C.: Prototypical contrastive learning of unsupervised representations. arXiv preprint arXiv:2005.04966 (2020)
19. Liu, B., Cao, Y., Lin, Y., Li, Q., Zhang, Z., Long, M., Hu, H.: Negative margin matters: Understanding margin in few-shot classification. In: European Conference on Computer Vision. pp. 438–455. Springer (2020)
20. Liu, J., Song, L., Qin, Y.: Prototype rectification for few-shot learning. In: European Conference on Computer Vision. pp. 741–756. Springer (2020)
21. Liu, Y., Lee, J., Park, M., Kim, S., Yang, E., Hwang, S.J., Yang, Y.: Learning to propagate labels: Transductive propagation network for few-shot learning. In: International Conference on Learning Representations (ICLR) (2019)
22. Liu, Y., Lee, J., Park, M., Kim, S., Yang, E., Hwang, S., Yang, Y.: Learning to propagate labels: Transductive propagation network for few-shot learning. In: International Conference on Learning Representations (2019)
23. Liu, Z., Lin, Y., Cao, Y., Hu, H., Wei, Y., Zhang, Z., Lin, S., Guo, B.: Swin transformer: Hierarchical vision transformer using shifted windows. arXiv preprint arXiv:2103.14030 (2021)
24. Manduchi, L., Chin-Cheong, K., Michel, H., Wellmann, S., Vogt, J.E.: Deep conditional gaussian mixture model for constrained clustering. arXiv preprint arXiv:2106.06385 (2021)
25. Miller, E.G., Matsakis, N.E., Viola, P.A.: Learning from one example through shared densities on transforms. In: Proceedings IEEE Conference on Computer Vision and Pattern Recognition. CVPR 2000 (Cat. No. PR00662). vol. 1, pp. 464–471. IEEE (2000)
26. Nichol, A., Schulman, J.: Reptile: a scalable metalearning algorithm. arXiv preprint arXiv:1803.02999 **2**(3), 4 (2018)
27. Qiao, L., Shi, Y., Li, J., Wang, Y., Huang, T., Tian, Y.: Transductive episodic-wise adaptive metric for few-shot learning. In: Proceedings of the IEEE/CVF International Conference on Computer Vision. pp. 3603–3612 (2019)
28. Rajeswaran, A., Finn, C., Kakade, S.M., Levine, S.: Meta-learning with implicit gradients. *Advances in neural information processing systems* **32** (2019)
29. Ravi, S., Larochelle, H.: Optimization as a model for few-shot learning (2016)
30. Ren, M., Triantafillou, E., Ravi, S., Snell, J., Swersky, K., Tenenbaum, J.B., Larochelle, H., Zemel, R.S.: Meta-learning for semi-supervised few-shot classification. arXiv preprint arXiv:1803.00676 (2018)
31. Rusu, A.A., Rao, D., Sygnowski, J., Vinyals, O., Pascanu, R., Osindero, S., Hadsell, R.: Meta-learning with latent embedding optimization. arXiv preprint arXiv:1807.05960 (2018)
32. Snell, J., Swersky, K., Zemel, R.: Prototypical networks for few-shot learning. *Advances in neural information processing systems* **30** (2017)
33. Sohn, K., Lee, H., Yan, X.: Learning structured output representation using deep conditional generative models. *Advances in neural information processing systems* **28**, 3483–3491 (2015)
34. Sun, Q., Liu, Y., Chua, T.S., Schiele, B.: Meta-transfer learning for few-shot learning. In: Proceedings of the IEEE/CVF Conference on Computer Vision and Pattern Recognition. pp. 403–412 (2019)
35. Sung, F., Yang, Y., Zhang, L., Xiang, T., Torr, P.H., Hospedales, T.M.: Learning to compare: Relation network for few-shot learning. In: Proceedings of the IEEE conference on computer vision and pattern recognition. pp. 1199–1208 (2018)
36. Tian, Y., Wang, Y., Krishnan, D., Tenenbaum, J.B., Isola, P.: Rethinking few-shot image classification: a good embedding is all you need? In: Computer Vision–ECCV

- 2020: 16th European Conference, Glasgow, UK, August 23–28, 2020, Proceedings, Part XIV 16. pp. 266–282. Springer (2020)
37. Vinyals, O., Blundell, C., Lillicrap, T., Wierstra, D., et al.: Matching networks for one shot learning. *Advances in neural information processing systems* **29**, 3630–3638 (2016)
 38. Wah, C., Branson, S., Welinder, P., Perona, P., Belongie, S.: The caltech-ucsd birds-200-2011 dataset (2011)
 39. Wang, Y., Chao, W.L., Weinberger, K.Q., van der Maaten, L.: Simpleshot: Revisiting nearest-neighbor classification for few-shot learning. arXiv preprint arXiv:1911.04623 (2019)
 40. Wang, Y., Xu, C., Liu, C., Zhang, L., Fu, Y.: Instance credibility inference for few-shot learning. In: *Proceedings of the IEEE/CVF Conference on Computer Vision and Pattern Recognition*. pp. 12836–12845 (2020)
 41. Xu, W., Wang, H., Tu, Z., et al.: Attentional constellation nets for few-shot learning. In: *International Conference on Learning Representations* (2020)
 42. Yang, L., Li, L., Zhang, Z., Zhou, X., Zhou, E., Liu, Y.: Dpgn: Distribution propagation graph network for few-shot learning. In: *Proceedings of the IEEE/CVF Conference on Computer Vision and Pattern Recognition*. pp. 13390–13399 (2020)
 43. Ye, H.J., Hu, H., Zhan, D.C., Sha, F.: Learning embedding adaptation for few-shot learning (2019)
 44. Yoon, J., Kim, T., Dia, O., Kim, S., Bengio, Y., Ahn, S.: Bayesian model-agnostic meta-learning. *Advances in neural information processing systems* **31** (2018)
 45. Yoon, S.W., Seo, J., Moon, J.: Tapnet: Neural network augmented with task-adaptive projection for few-shot learning. In: *International Conference on Machine Learning*. pp. 7115–7123. PMLR (2019)
 46. Yu, M.H., Li, J., Liu, D., Zhao, D., Yan, R., Tang, B., Zhang, H.: Draft and edit: Automatic storytelling through multi-pass hierarchical conditional variational autoencoder. In: *Proceedings of the AAAI Conference on Artificial Intelligence*. vol. 34, pp. 1741–1748 (2020)
 47. Zagoruyko, S., Komodakis, N.: Wide residual networks. arXiv preprint arXiv:1605.07146 (2016)
 48. Ziko, I., Dolz, J., Granger, E., Ayed, I.B.: Laplacian regularized few-shot learning. In: *International Conference on Machine Learning*. pp. 11660–11670. PMLR (2020)
 49. Zintgraf, L., Shiarli, K., Kurin, V., Hofmann, K., Whiteson, S.: Fast context adaptation via meta-learning. In: *International Conference on Machine Learning*. pp. 7693–7702. PMLR (2019)